

SYNTHESIS AND CHARACTERIZATION OF ACTIVATED CARBON FROM MAHOGANY FRUIT SHELL (*Khaya senegalensis*) IMPREGNATED WITH TiO_2 USED IN THE ADSORPTION OF CADMIUM AND ARSENIC

Abstract

*In this Study, low-cost activated carbon impregnated with TiO_2 (Ac/ TiO_2) was prepared from mahogany fruit shell (*Khaya Senegalensis*) by chemical activation using phosphoric acid, H_3PO_4 . This resulting product was evaluated for the removal of Arsenic and Cadmium ions from aqueous solutions. The prepared activated carbon was characterized using SEM, FTIR and XRD. Operational parameters such as initial concentration, adsorbent dose, contact time, effects of pH and temperature were studied in a batch system. It was found that the percentage removal for arsenic and cadmium were 99.99% and 99.78 respectively. Equilibrium of the adsorption processes were obtained by testing the adsorption data using two different isotherm models: Langmuir and Freundlich. The adsorption of arsenic fitted well with Freundlich with R^2 value of 0.9106. The kinetic of adsorption process was tested through pseudo first order and pseudo second order models. The Pseudo Second Order Kinetic Model provides the best correlation for the experimental data of both the two metals studied. Thermodynamics parameters, such as ΔG^0 , ΔH^0 and ΔS^0 were also calculated. This result shows that the process of adsorption for As was spontaneous and exothermic, while that of cadmium was spontaneous and endothermic.*

Keywords Activated carbon, adsorption studies, impregnation, khaya senegalensis, kinetics

1. Introduction

Heavy metals are among the most investigated environmental pollutants. Almost every heavy metal and metalloid may be potentially toxic to biota depending upon the dose and duration of exposure. Many elements are classified into the category of heavy metals, but some are relevant in the environmental context. List of the environmentally relevant most toxic heavy metals and metalloids contains Cr, Ni, Cu, Zn, Cd, Pb, Hg, and As[1]. Heavy metals are naturally occurring elements that have a high atomic weight and a density at least 5 times greater than that of water. Their multiple industrial, domestic, agricultural, medical and technological applications have led to their wide distribution in the environment; raising concerns over their potential effects on human health and the environment. Their toxicity depends on several factors including the dose, route of exposure, and chemical species, as well as the age, gender, genetics, and nutritional status of exposed individuals.

Some of the methods of removing these metals include chemical precipitation, membrane filtration, ion exchange, reverse osmosis, liquid extraction on electro-dialysis [2]. These processes however, have considerable disadvantages including incomplete metal removal especially at low concentrations, requiring expensive equipment and monitoring systems, large number of reagents or energy requirements and generation of toxic sludge or other waste

products that require disposal [2]. Therefore, the search for new technologies for the removal of heavy metals from aqueous media has been directed towards adsorption as a cost-effective and eco-friendly technique used in waste water treatment over the last few decades [3].

Adsorption is widely used as an effective method of removing wide range of dissolved pollutants (organics or inorganic) in an effluent. Activated carbon (AC) is a well-known adsorbent that can be used efficiently for the removal of a broad spectrum of pollutants from air, soil and liquids. Adsorbents are usually porous solids, and adsorption occurs mainly on the pore walls inside particles. Examples are activated carbon (adsorbs mainly organics), silica gel and activated alumina (absorb moisture), zeolites and molecular sieves and synthetic resins. Among them, AC is a more efficient adsorbent for elimination of many pollutants (organic, inorganic, and biological) of concern in water and wastewater treatment. AC is a broad-spectrum agent that effectively removes toxic and bio-refractive substances such as insecticides, herbicides, chlorinated hydrocarbons, heavy metal ions, and phenols, typically present in many water supplies [5]. AC in fact is a microcrystalline, non-graphitic form of carbon with porous structure that has been processed to develop its internal porosity. AC has a high degree of porosity, an extensive surface area, and a high degree of surface reactivity [4].

Activated Carbon (AC) is a tasteless solid, micro crystalline non-graphitic form of black carbon material with a porous structure [6]. It has been regarded a unique and versatile adsorbent because of its extended surface area, micro porous structure, high adsorption capacity and high degree of surface reactivity [6]. Commercial adsorbents that have been used in large scale adsorptive separation and purification processes include activated carbon, zeolite, activated alumina, silica gel, and polymeric adsorbent were reported to be very expensive compare to some of the agricultural by product that were mention above which are inexpensive and available in our environment as waste which have been discovered to be good sources of activated carbon [7]. The use of activated carbon in industry is very important and requires a solid having a very developed porous structure. Researchers have reported that organic matter (Biomass) is effective for the preparation of such activated carbon with highly porous structure. Synthetic activated carbons usually prepared from petroleum sources are expensive and non-biodegradable and therefore pose problems of environmental pollution after use [8]. Impregnation of AC with TiO_2 enhances the efficiency of AC. TiO_2 can effectively enhance energy absorption, promote electronic transition, produce more electron-hole pairs, and reduce the recombination of electron-hole pairs [9].

2. MATERIALS AND METHODS

2.1 Reagents

The reagents used were; phosphoric acid, distilled water, deionized water TiO_2 , arsenic oxide and cadmium nitrate.

2.2 Analytical Equipment and Apparatus

Fourier Transform Spectroscopy (FTIR- 84008), SEM, XRD, AAS, Vacuum pump/Buchner funnel, Oven (Thermostat oven DHG-9023A), Muffle Furnace, Weighing Balance, pH Meter, sieve, beakers, measuring cylinder, conical flask, petri dishes, pestle and mortar, trays, crucibles, tongs, water bath (Grant JB Series) and spatula.

2.3 Sample Collection and Preparation

The mahogany fruit shell samples were collected within the premises of Gombe State University campus. The collected samples were then washed with distilled water to remove unwanted particles. After that, the sample was dried in an oven at 120°C for 4h. The dried raw material was ground to particle size of 250µm. The particle size was determined using a laboratory test sieve.

2.4 Chemical Activation and Carbonization

The dried Mahogany Fruit Shells (MFS) material was soaked in a boiling solution of 40 % H_3PO_4 for one hour and kept at room temperature for 24 hours. After that, the pith was separated, air dried and carbonized in muffle furnace at 400°C. Then the materials were washed with plenty of water to remove residual acid, dried at 110 °C in an oven and stored in a tight lid container for adsorption studies[10].

2.5 Impregnation with TiO_2

The carbonized activated carbon was impregnated with 10% TiO_2 to enhance the selective adsorption capacity of the adsorbent [11].

2.6 Characterization

MHFS was characterized using Fourier Transform Spectroscopy (FTIR), Scanning Electron Microscopy (SEM) and X-Ray Diffraction (XRD) Analysis.

2.6.1 Fourier Transform Spectroscopy (FTIR- 8400s)

FTIR analysis was done to determine the functional groups present in the samples before and after impregnation with TiO_2 .

2.6.2 Scanning Electron Microscopy (SEM)

This was done in order to determine the structure and external morphology of the activated carbon samples before and after impregnation with TiO_2 .

2.6.3 X-Ray Diffraction (XRD) Analysis (X-Pert Plus)

XRD analysis was done to find out the average crystalline size. The Debye Scherrer equation was used to calculate the average crystalline size. The Debye Scherrer equation is as follows:

$$D = K\lambda/\beta\cos\theta$$

Where D= Particles size = 0.94

K= Constant volume

λ = X-ray wavelength(0.154nm)

β =Line broadening at half the maximum intensity

θ = Braggs angle(in degree).

2.7. Preparation of Stock Solutions

The stock solution of the metal ions for the adsorption tests was prepared in stock solutions of up to 1000 mg/L.

2.8. Preparation of Metals (As & Cd) Solution

A stock solution of metal ions was prepared by dissolving 2.641g of arsenic oxide in 20ml of 20% sodium hydroxide and 10ml of sulphuric acid in 1000ml volumetric flask was added,

shaken and then the volume was made up to marked point. Also, 2.103g of cadmium nitrate was dissolved in 1000ml volumetric flask, shaken and the volume was made up to the marked point respectively.

2.9 Batch Adsorption Experiment

Batch adsorption experiment was used in investigating the effect of initial concentration, adsorbent dose, contact time, temperature and pH.

2.9.1 Effect of Adsorbent Dose

The effect of adsorbent dose on the adsorption process was studied by increasing the mass of the adsorbent from 0.1, 0.2, 0.3, 0.4 and 0.5g in a 250 mL volumetric flask containing 25 ml solution of metals.

2.9.2 Effect of pH

The effect of solution pH was monitored by changing the initial pH of the solutions from 3 to 11. The pH was adjusted by using 0.1 M hydrochloric acid or 0.1 M sodium hydroxide and measured using a pH meter (Mettles Toledo, Model: Ross FE 20, USA).

2.9.3 Effect of Temperature

The effect of solution temperature on the adsorption process was studied by varying the adsorption temperature at 10, 20, 30, 40, 50 and 60 °C by using the temperature control system of the water bath (Grant JB series), while other process parameters such as adsorbent dosage, agitation speed, pH and volume of the solution remained constant.

2.9.4 Effects of Initial Concentration

The effect of initial concentration on the adsorption process was analyzed by varying the concentrations at 5, 10, 15, 20 and 25 (mg/L).

2.9.5 Effect of Contact Time

The effect of contact time was also studied by varying the time from 10, 20, 30, 40 and 50 min. with continuous shaking by agitation at 120 rpm.

3.8 Data Evaluation (As & Cd)

The percentage removal of Cadmium and arsenic and the amount adsorbed (mg/g) were calculated using the following equations;

$$\% \text{ Removal} = \frac{C_i - C_e}{C_i} \times 100 \quad (1)$$

$$q_e = \frac{(C_0 - C_e)V}{W} \quad (2)$$

Where; C_i is the initial concentration of the metals solution (mg/L).

C_e is the equilibrium concentration of the metals solution (mg/L).

C_0 is the initial concentration of the adsorbent.

W is the mass of adsorbent (g)

V is the volume of the solution (L)

2.10 Adsorption Isotherms

The equilibrium data were fitted to Langmuir and Freundlich isotherm models.

2.10.1 Langmuir Isotherm

The Langmuir isotherm was used to obtain the maximum adsorption capacity produced from complete monolayer average of adsorbent surface.

$$C_e/q_e = C_e/q_m + 1/q_m K_L \quad (3)$$

Where

q_e is the equilibrium dye concentration on the adsorbent (mg g^{-1});

C_e is the equilibrium dye concentration in solution (mg L^{-1});

q_{max} is the monolayer capacity of the adsorbent (mg g^{-1});

K_L is the Langmuir constant.

The plot of (C_e/q_e) Vs C_e should yield a straight line if the Langmuir equation is obeyed by the adsorption equilibrium. The slope and the intercept of this line then give the values of constant q_m and K_L .

A further analysis of the Langmuir equation can be made on the basis of a dimensionless equilibrium parameter, R_L , known as separation factor given by equation = (4)

$$R_L = \frac{1}{1 + K_L C_0} \quad (4)$$

The value of R_L lies between 0 and 1 for a favorable adsorption, while $R_L > 1$ represents an unfavorable adsorption, and $R_L = 1$ represents the linear adsorption, while the adsorption operation is irreversible if $R_L = 0$.

2.10.2 Freundlich Isotherm

For adsorption from solution, the Freundlich isotherm is expressed as given by equation (5):

$$\text{Log } q_e = \text{Log } K_f + 1/n \text{ Log } C_e \quad (5)$$

Where

K_F (mg/g) and n are the Freundlich constants related to adsorption capacity and intensity, respectively.

A linear plot of $\text{Ln } q_e$ vs $\text{Log } C_e$ gives K_F and n values.

2.11 Adsorption Kinetics

The kinetics of removal of metals was explained by using pseudo first order and second-order models.

2.11.1 Pseudo First Order Kinetics

The non-linear form pseudo first-order equation is given by equation

$$\text{Log } (q_e - q_t) = \log q_e - \frac{K_1}{2.303} t \quad (6)$$

Plot of $\log \log (q_e - q_t)$ Vs t gives a straight line for the first order adsorption kinetics, which allows the computation of the adsorption rate constant. K_1

2.11.2 Second-Order Kinetics

Application of the second order kinetics has to be tested with the rate equation given by equation (7):

$$\frac{t}{qt} = \frac{1}{K_2 q_e^2} + \frac{1}{q_e} t \quad (7)$$

Where, q_e is the maximum adsorption capacity (mg g^{-1}), qt is the amount of metal ion adsorbed at time t (mg g^{-1}) and k_2 is the pseudo-second order kinetic rate constant ($\text{g mg}^{-1} \text{min}^{-1}$). The plot of t/qt vs t should give a linear relationship, which allows the computation of q_e , and k_2 .

3.RESULT AND DISCUSSION

3.1 Characterization of The Adsorbent

The adsorbent was characterized using FTIR, SEM and XRD analysis.

3.1.1 FTIR Analysis of the Adsorbent

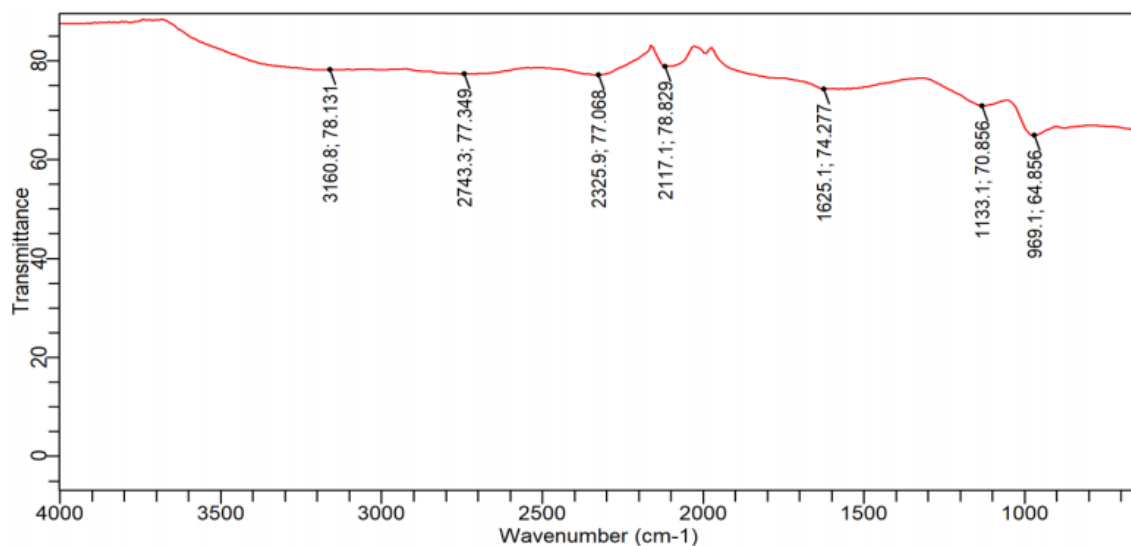


Fig. .1: FTIR Analysis of the Unimpregnated MHFS

The FTIR spectra of the prepared unimpregnated activated carbon displayed in Fig..1 shows several peaks. The peak at 3160.8 cm^{-1} , represent O-H stretching H-bonded due to alcohol/phenols 2743.3 cm^{-1} , represent C-H stretching due to the alkane 2325.9 cm^{-1} and 2117 cm^{-1} represent $\text{C}\equiv\text{C}$ triple bond stretching due to the alkynes, 1625 cm^{-1} , C=C due to conjugate alkene 1133 cm^{-1} , indicate C-O stretching due to tertiary alcohol or either, 969.1 cm^{-1} C=C due to bending alkene.

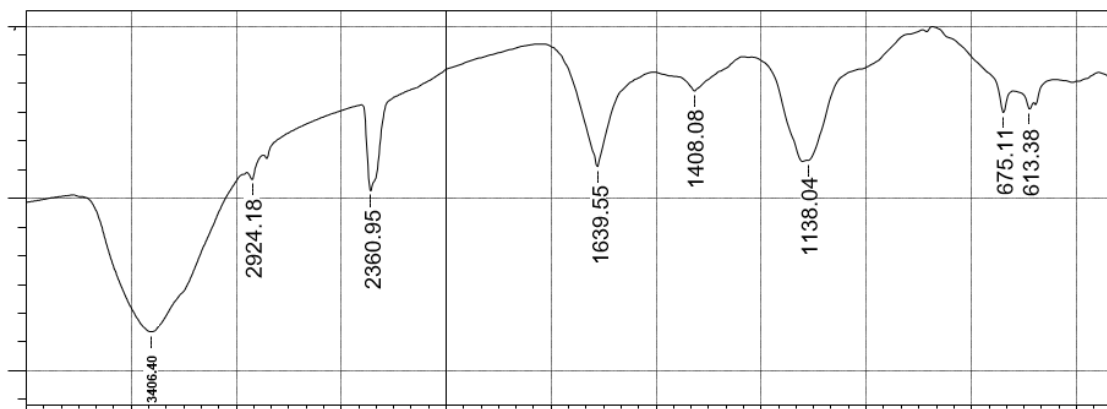


Fig. 2: FTIR Analysis of the Impregnated MHFS

The FTIR spectra of the prepared impregnated activated carbon displayed in Fig. 2 shows. The peak at 3406.40 cm^{-1} , represent O-H stretching H-bonded due to alcohol/phenols 2924.18 cm^{-1} , represent C-H single bond stretching due to the alkanes 2360.95 cm^{-1} , represent $\text{C}\equiv\text{C}$ triple bond stretching due to the alkynes, 1408.08 cm^{-1} , C-C (in ring) 1138.04 cm^{-1} , indicate C-O stretching due to tertiary alcohol or ether, 678.11 cm^{-1} and 613.38 cm^{-1} indicate C-H single bond due to alkyne bend respectively.

3.2. SEM Analysis of the Adsorbent

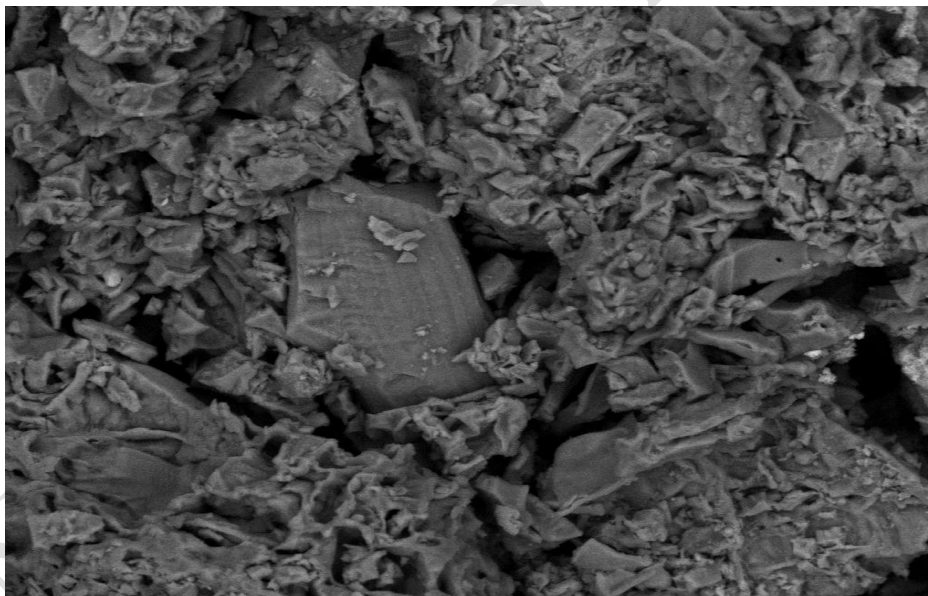


Fig. 3: SEM of the unimpregnated MHFS

SEM Image of the unimpregnated activated carbon particles in Figure 3 showed cavities, pores and more rough surfaces on the carbon samples. The surface is pitted and fragmented due to the carbonization with H_3PO_4 and activation process [12].

3.2 SEM Analysis of the Adsorbent

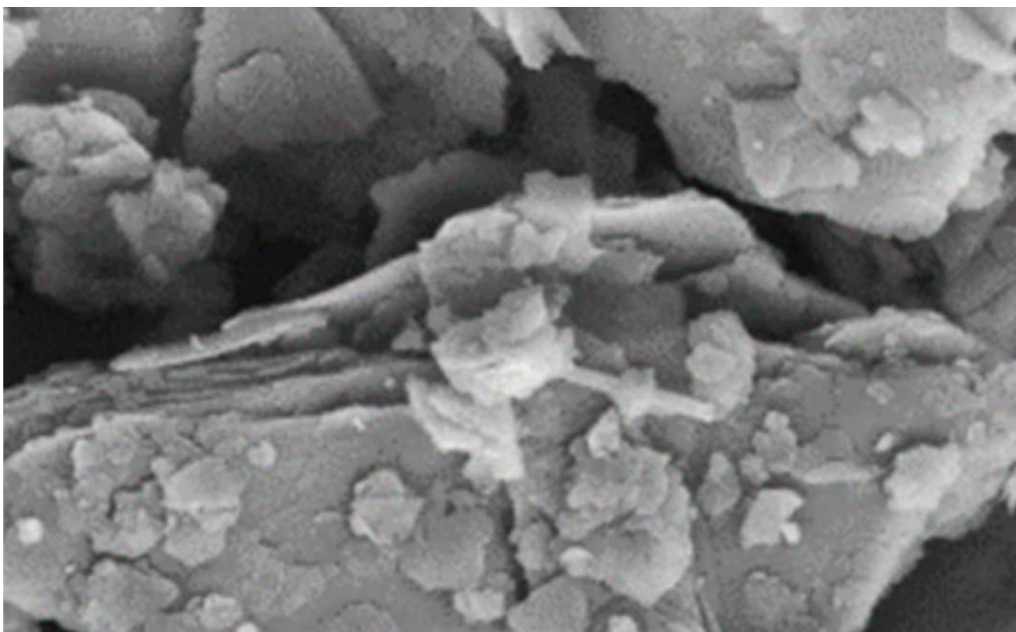


Fig. 4: SEM of the impregnated MHFS

The SEM image in Figure 4 shows pores on the rough surface of the impregnated activated carbon. However, a large number of various sizes and shapes pores observed, with particles evenly distributed and homogeneous. It is remarkable that porous material having a high specific surface area should play an important role of providing the suitable binding sites for heavy metals ions in the process of removal from aqueous solution. [13].

3.3 XRD Analysis of Adsorbent

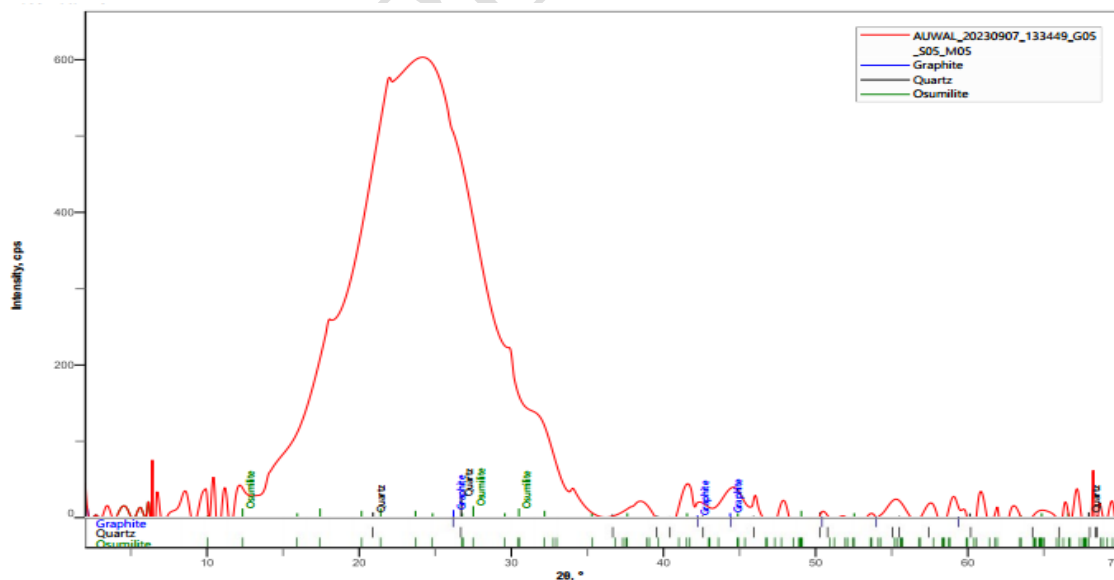


Fig. 5: XRD Analysis of the unimpregnated MHFS

From Figure 5, the XRD result shows a long prominent peak observed at $2\theta=24.06$ with respect to the plane of (III). It shows face centered cubic structure and the average crystalline size 61.1 nm as calculated by the Scherer equation. [14].

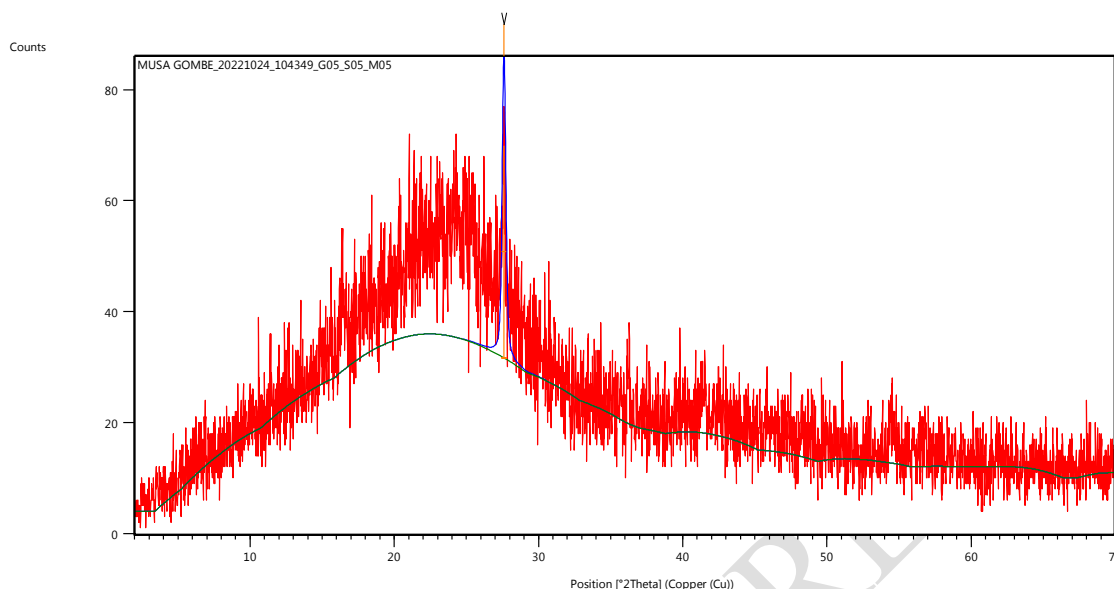


Fig. 6: XRD Analysis of the impregnated MHFS

From Figure 6 the result obtained from the XRD analysis of the prepared activated carbon with the brags angle of between $127.59-38.19^\circ$ observed along with the weak peaks, it was found that, one prominent peak was observed at $2\theta = 27.59^\circ$ with respect to the plane of (111). It shows Face Centered Cubic structure and the average crystalline size 31.64nm. According to the Scherer equation calculated, the result obtained is nearly in agreement to the literature reported by [14].

4.2 Adsorption Studies

4.2.1 Effect of Concentration

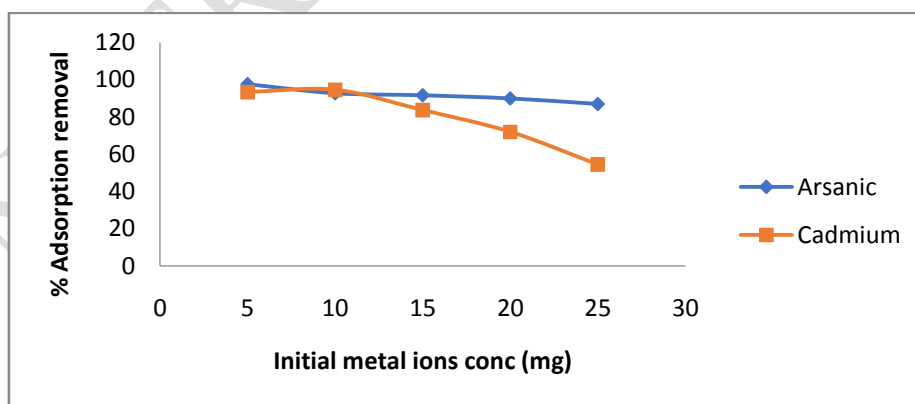


Fig. 7: Effect of initial concentration

The effects of initial concentration on the adsorption of the metal ions (As & Cd) were investigated at the range of 5-25mg/L while other parameters were kept constant. The results

obtained are presented in Figure 7. It is clear from Figure 7 that the percentage removal of the metal ions decreases with increases in initial concentration of the solution.

At the lower metal ions concentration, the percentage uptake was higher due to larger surface area of the adsorbent being available for adsorption when the concentration of the metals ions becomes higher the percentage removal decreased since the available site for adsorption became less due to saturation of adsorption site [15].

4.2.2 Effect of Adsorbent

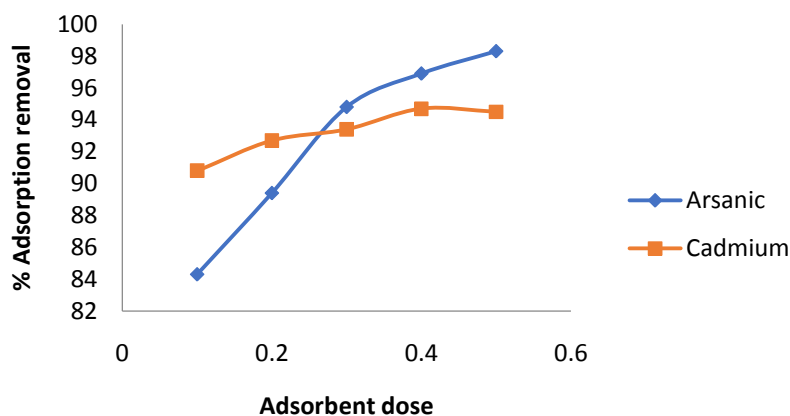


Fig. 8: Effect of adsorbent dose

Adsorbent dosage is another major factor which is used to determine the ability of the adsorbent, in order to assess the effect of the adsorbent dose. The effect of adsorbent dose on the removal of the As^{3+} and Cd^{2+} was investigated at various the range of 0.1-0.5. The results obtained are presented in Figure 8. The percentage removal of the metals ions increase with increase in adsorbent dose, the increase in percentage removal of the metals ions with increase in adsorbent dose is obviously due to the availability of larger adsorption sites due to increase dose. It is obvious that with increase in amount of the active site, there is an increase in removal efficiency[16].

4.2.3 Effect of pH

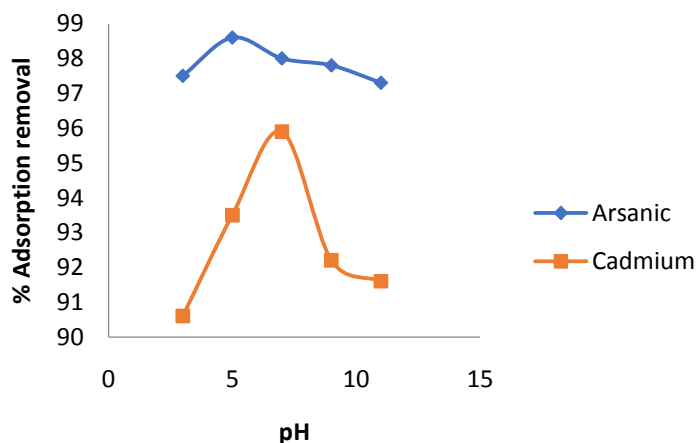


Fig. 9: Effect of pH

The pH of an aqueous solution is described as significant parameters that influence the adsorption process. The effects of pH on adsorption of the metal ions (As & Cd) were investigated at pH range of 3 – 11 other parameters were kept constant. The results obtained are shown in Figure 9. Figure 9 shows that the maximum adsorption of arsenic was obtained at a pH of 5 which related to the finding of [17] which states that the adsorption of As in acid medium is more effective while the maximum adsorption of Cd was obtained at pH of 7. This is in agreement with the result of [18]

4.2.4 Effect of Temperature

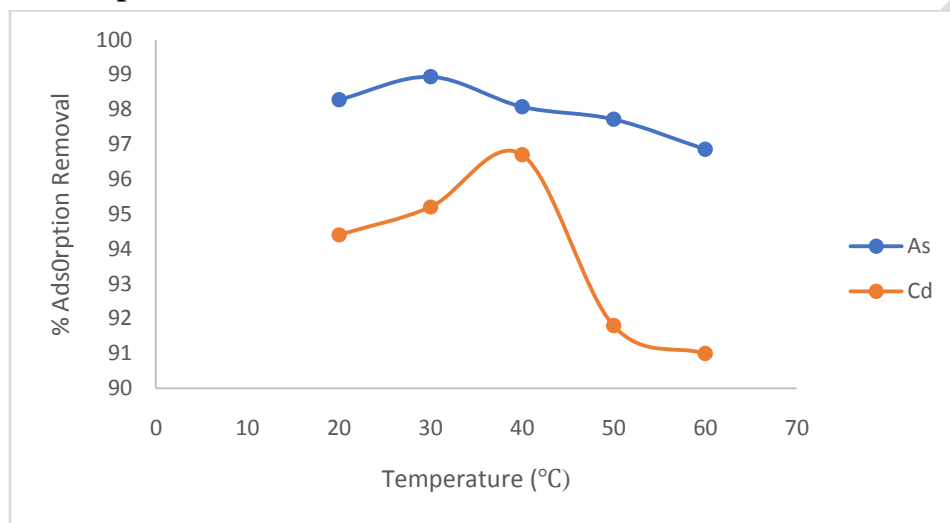


Fig. 10: Effect of temperature

The effect of temperature was carried out by varying the temperature from 10 – 60 °C while other parameters were kept constant. From the results in Figure 10, it is clear that the maximum adsorption of As was found to be at 30 °C while the maximum adsorption of Cd was found to be at 40 °C after that the adsorption decreases. This is in agreement with the findings of [18] which states that the decrease in adsorption may be due to the endothermic nature of the adsorption; also, the increase of metal ions could be a result of increase in mobility of the metal ions present in the system.

4.2.5 Effect of Contact Time

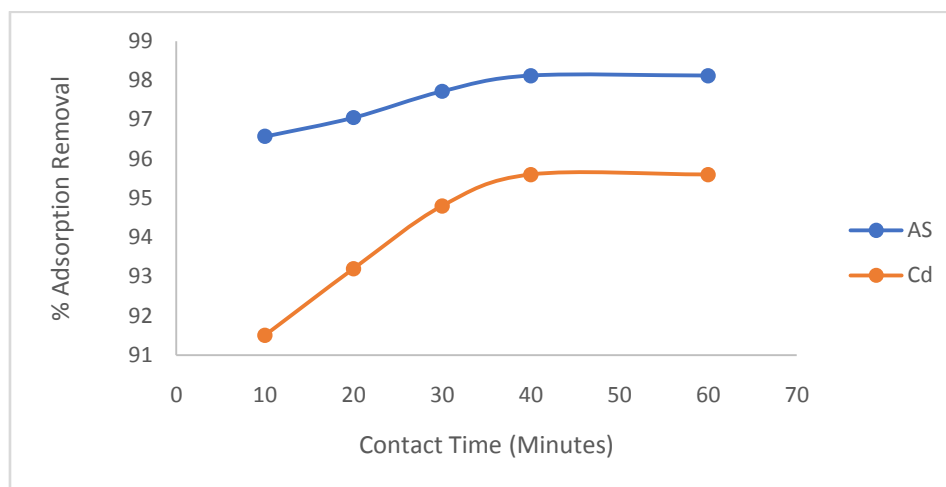


Fig. 11: Effect of contact time

It is well documented that contact time is a major parameter because it defines the equilibrium period during the process of adsorption. It is well known that, the characteristics of adsorbent and its free adsorption attain equilibrium. In this work the adsorption of metals ions was experienced as a function of time in the interval of 10 – 60min and the results are presented in Fig. 11. It is observed that adsorption for metal ions take place at very rapid rate and followed by slower adsorption rate. This is because initially all adsorbent sites were vacant and later concentration gradient was high later the percentage removal rate decreased significantly resulting from saturation of the activated carbon [13].

4.3 Adsorption Isotherm

The adsorption isotherm gives a picture of the distribution of adsorbent species between on aqueous and solid phase. The experimental data were analyzed using Langmuir and Freundlich as the two most commonly used Isotherm models. Adsorbent surface may be monolayer or multilayer depending up on the model which are followed by the data. Monolayer adsorption can be well explained by Langmuir model while Freundlich model is used to explain multilayer adsorption of adsorbed molecule on heterogenous surface. Table 1 gives the overall summaries of Langmuir and Freundlich models for As (MHFS) with R^2 values of (0.9007) which show that the experimental data fit well with Freundlich model [21]. While for Cd (MHFS) the values of R^2 was (0.9106) which indicate that Langmuir was better fitted than Freundlich Isotherm this in agreement with [16].

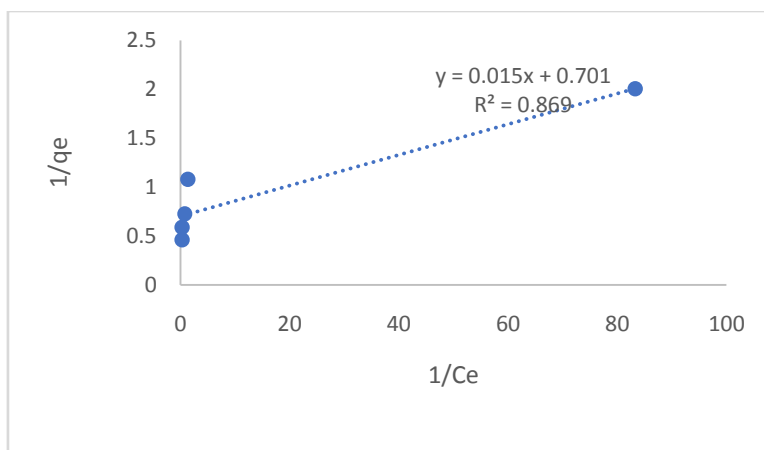


Fig. 12: Langmuir for As on MHFS

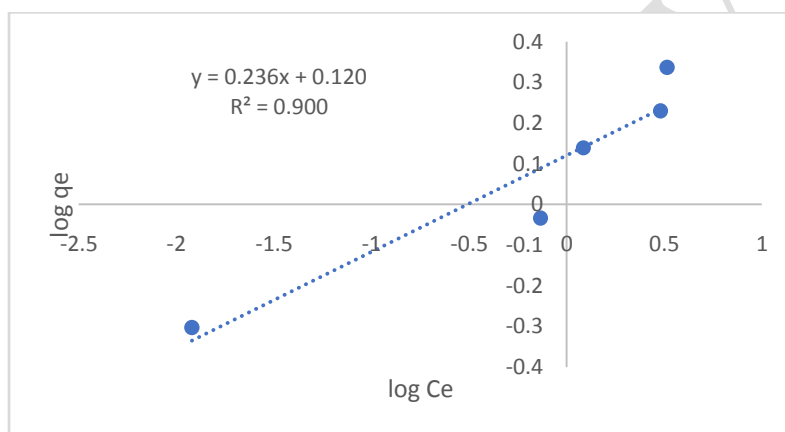


Fig. 13: Freundlich for As on MHFS

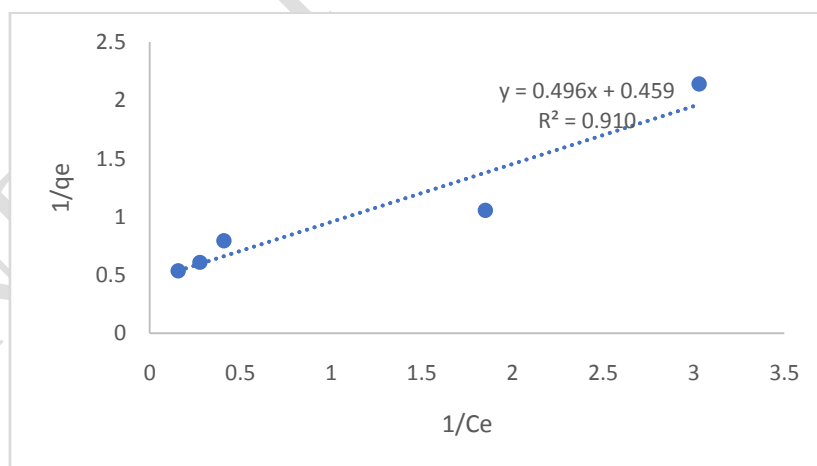


Fig. 14: Langmuir for Cd on MHFS

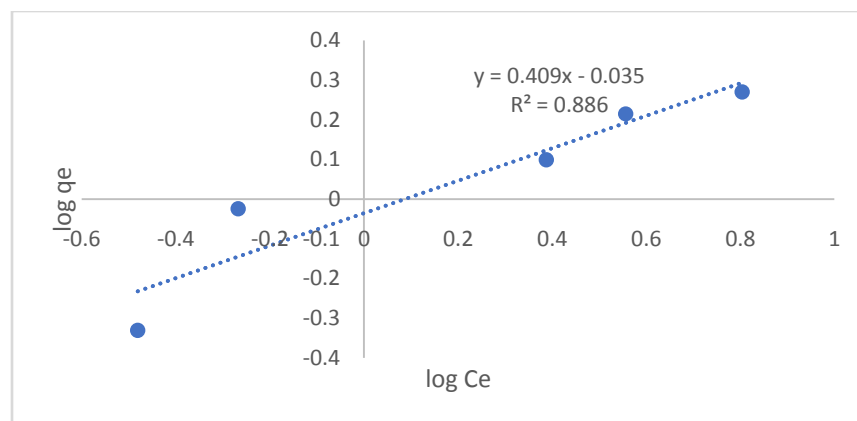


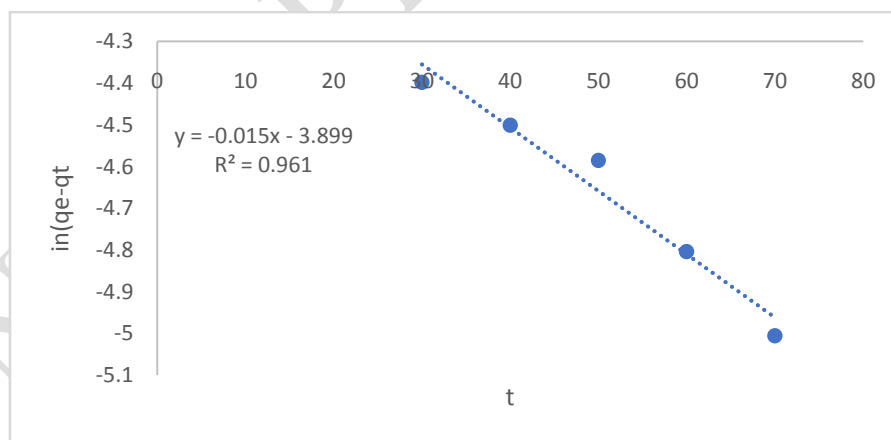
Fig. 15: Freundlich for Cd on MHFS

TABLE 1: Isotherm of Adsorption Study on MHFS

Isotherm Model Result	Metal ions	
	As	Cd
Langmuir	q_m	1.42572
	K_L	2.174859
	R^2	0.926456
Freundlich		0.9106
	K_F	1.319168
	$1/n$	0.920662
	R^2	0.381
		0.8867

4.4 Kinetic Study

The adsorption kinetics of each heavy metal ion determined under precise time condition was performed. The kind of adsorption process depends on physico-chemical characteristic of the adsorbent and system status like temperature. The linear graph of pseudo-first order was plotted from $\ln(q_e - q_t)$ against t (mins) and the graph of pseudo-second order was plotted from t/q_t against t (min). From the results obtained, pseudo-second order correlated well with the experimental data better than pseudo-first order. The R^2 from pseudo-second order was much higher than that of pseudo first order and also the theoretical and experimental values are in a good correlation with each other. By contrast, in the pseudo second order model, the calculated $q_e(\text{cal})$ values are very close to $q_e(\text{exp})$, and the R^2 values converge to 1, indicating the validity of the pseudo second order, with this we can say that pseudo second order is best fitted for the adsorption, the result is similar to obtained by [20].

**Fig. 16: Pseudo First Order As on MHFS**

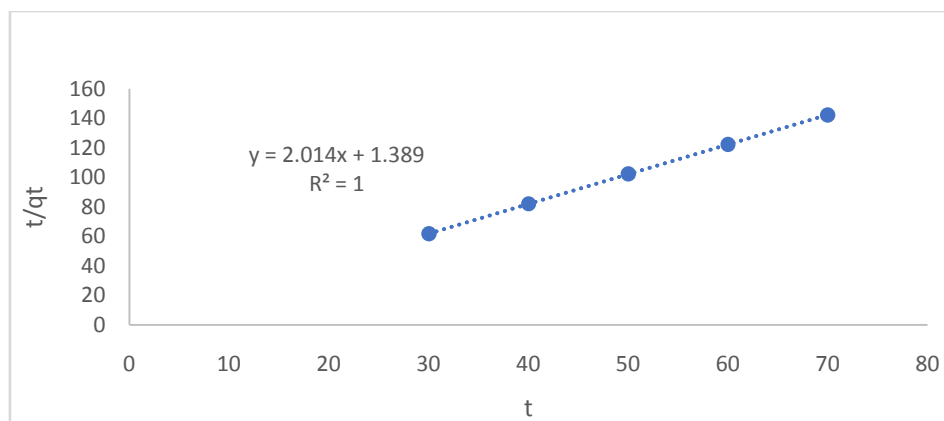


Fig. 17: Pseudo Second Order for As on MHFS

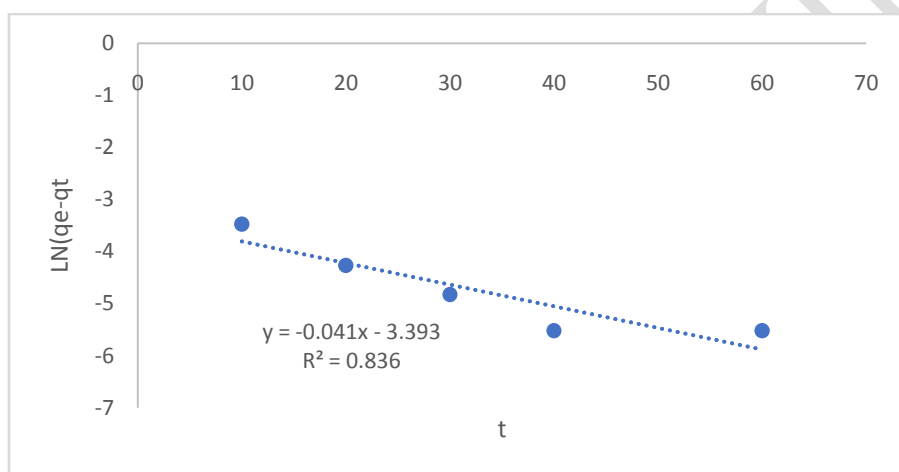


Fig. 18: Pseudo First Order for Cd on MHFS

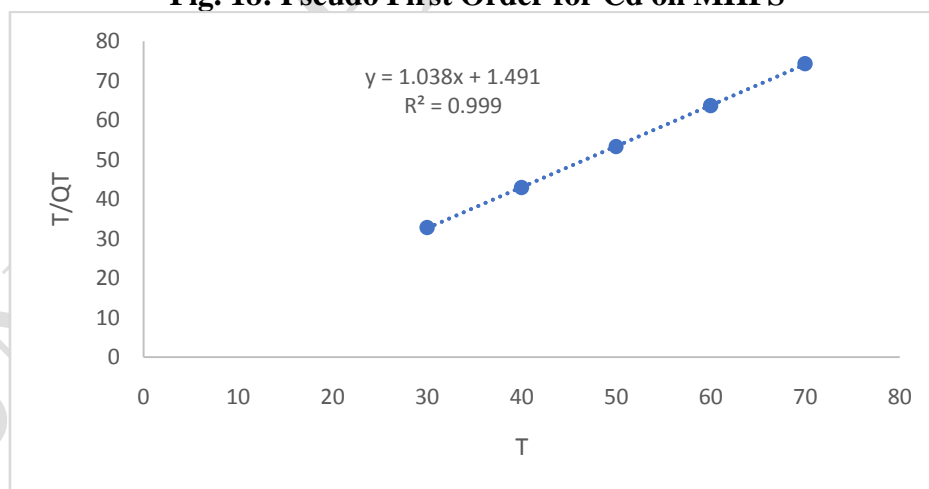


Fig. 19: Pseudo Second Order for Cd on MHFS

Table 2: Kinetics of Adsorption Study on MHFS

Kinetic Study	Metal ions	
	As	Cd
Pseudo-firstorder		
	q_{exp}	0.499
	$q_{e_{cal}}$	0.020
	K_1	0.0152
Pseudo-second order	R^2	0.9616
	$q_{e_{cal}}$	0.496401
	K_2	0.246414
	R^2	1

4.5 Thermodynamic Study

Thermodynamic parameters are properly assessed; they provide in-depth information regarding the inherent energy and structural changes after adsorption. ΔG is the change in free Gibbs energy (kJmol^{-1}), R is the universal gas constant ($8.314 \text{ Jmol}^{-1}\text{K}^{-1}$), K_e is the thermodynamic equilibrium constant and T is the absolute temperature (K). The values of ΔH and ΔS were determined from the slope and the intercept from the plot of $\ln K_e$ against $1/T$ (K^{-1}) in Tables 1 and 2 above which show the summary. The negative value of the Gibbs free energy (ΔG^0), obtained from arsenic and cadmium indicated that the adsorption process is spontaneous in nature. For arsenic, ΔH is negative which indicated that the reaction is exothermic, ΔS^0 was also negative indicating that there are less degree of randomness while for cadmium, ΔH is positive which means that the reaction is endothermic, also ΔS^0 was positive indicating that there is high degree of randomness.

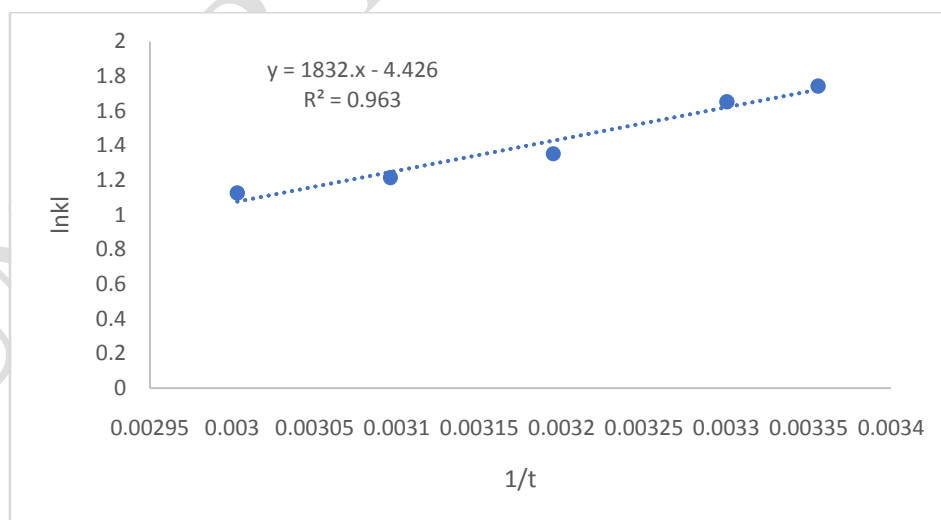
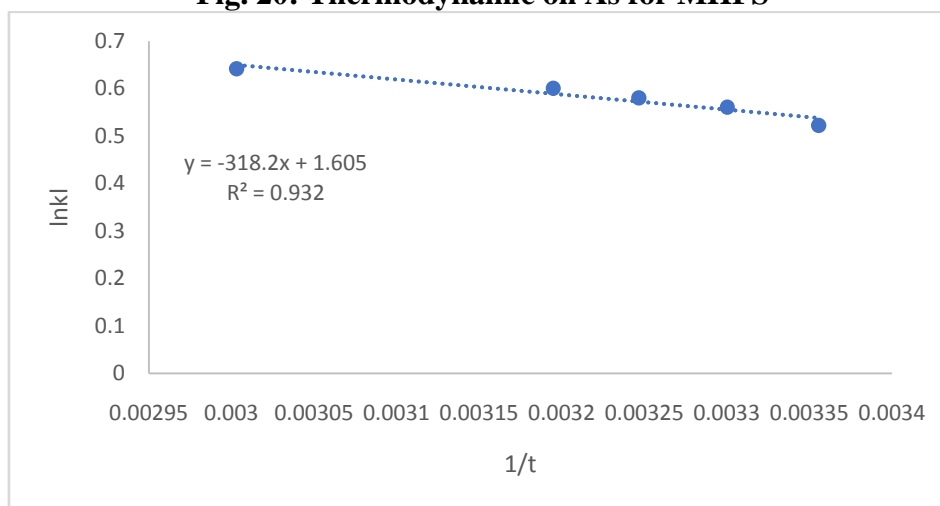


Fig. 20: Thermodynamic on As for MHFS**Fig. 21: Thermodynamic on Cd for MHFS****TABLE 3: Thermodynamic Study on MHFS**

Model	Metal ions	
	As	Cd
$-\Delta G^\circ$ (KJ.mol ⁻¹)	20°C	4.31819
	30°C	4.16246
	40°C	3.52038
	50°C	3.26432
	60°C	3.11867
		1.29376
ΔH° (KJ.mol ⁻¹)		1.41242
		1.48629
ΔS° (J.mol ⁻¹ .K ⁻¹)		1.56274
		1.77701
	-15.231.2	26.45515
	-36.8044	13.35062

CONCLUSION

Based on this experimental research the impregnated activated carbon (Ac/TiO₂) was taken into consideration in removing arsenic and cadmium from solutions containing the metals ions. The adsorption experiments were studied under the following parameters: Initial concentration, adsorbent dose, contact time, temperature and pH of the adsorbent prepared solution.

These experiment studies the efficiency of each parameter in the removal of arsenic and cadmium from a solution. The optimal percentage removal for arsenic was 99.99% at 5mg/L with 0.5g adsorbent dose while that of cadmium was 99.78% with 0.5g adsorbent dose at 10mg/L.

Therefore, activated carbon impregnated with TiO₂ prepared from mahogany fruit shells would be useful for the economic treatment of water containing some heavy metals ions such as arsenic and cadmium ions because of its outstanding adsorption capacity.

REFERENCE

1. Kemal A, Siraj K, and Michael WH. Adsorption of Cu (II) and Cd(II) onto activated carbon prepared from pumpkin seed shell. *Journal of Environmental Science and pollution research*. 2009; **47**(3): 257 – 264.
2. Kumar R, Obrai S, and Sherma A. Biosorption of Heavy Metals Ions Using Modified Waste Tree Bark Material. *Journal of Environmental Sciences*. 2012;**3**(1): 720-726
3. EngilaJM, Dauda BE, Iyaka, YA, and Jimoh T. Agricultural waste as low-cost adsorbent for heavy metal removal from waste water, *International Journal of Physical Science*. 2011;**6**(8): 1252 – 2157
4. Ansari R, and Sadegh M. Application of Activated Carbon for Removal of Arsenic Ions from Aqueous Solutions, *E – Journal of Chemistry*. 2007;**4**(1) 103-108.
5. Mohammad-Khan A, and Ansari R. Activated Charcoal: Preparation, Characterization and Applications: A Review Article. *International Journal of ChemTech Research*. 2009;**1**(4): 859-864.
6. Sugumaran P, Susan V, Ravichandran and Seshadri S. Production and Characterization of Activated Carbon from Banana Empty Fruit Bunch and Delonix Regia Fruit Pod. *Journal of Sustainable Energy and Environment*. 2012;**3**: 125-132.
7. Alau K Gimba C, Kagbu J, and Nale B. Preparation of Activated Carbon from Neem (*Azadirachta indica*) Husk by Chemical Activation with H_3PO_4 , KOH and $ZnCl_2$, *Archives of Applied Science Research*. 2010;**2**(5): 451-455.
8. Abba C, Abdoul W, GastonZ, AbdoulN and Divine B. Bleaching of Natural Cotton Seed Oil Organic Activated Carbon in Batch System: Kinetics and Adsorption Isotherms. *Processes*. 2018; **6**(22): 10-3990
9. Jin X, Che R, Yang J, Liu Y, ChenX, JiangY, Liang J, Chen S and Su H. Activated Carbon and Carbon Quantum Dots/Titanium Dioxide Composite Based on Waste Rice Noodles: Simultaneous Synthesis and Application in Water Pollution Control. *Nanomaterials*. 2022; **12**(3), 472.
10. Azza E, Nahla AT and Asmaa MA. Preparation of activated carbon (Chemically and physical) from Banna pith for heavy metal removal from waste water. *Sci-Afric Journal of Scientific Issues, Research and Essays*. 2014;**2**(9): 399-403.

11. Hidayua AR and Muda N. Preparation and characterization of impregnated activated carbon from palm kernel shell and coconut shell for CO₂ capture International Conference on Process Engineering and Advanced Materials Procedia Engineering. 2016;**148**: 106 – 113
12. RafficaBaseri J, Palanisamy PN and Sivakumar P.Preparation and Characterization of Activated Carbon from Textile Waste Water. Advances in Applied Sciences Research. 2012;**3** (1): 377-383
13. Bedmohata MA, Chandari AR, Singh SP and Choudhary MD. Adsorption Capacity of Activated Carbon Prepared by Chemical Activation of Liginin for the removal of Methylene Blue dye. International Journal of Advance Research and Chemical Science. 2015;**2**(8): 1-13
14. Athifeona T, Sabeena G, Pushpalaksmi E, Jenson S and Annadurai G. Synthesis and Characterization of ZnO-MMT Nanocomposites for Antibacterial Activity Studies. Journalof applied science and Environmental Management. 2020;**24**(6): 1079-1089
15. AugustineAU, Ishaq B, Akpomie TM and Edoh R. Removal of Lead (II) amd Iron (II) Ions From Aqueous Solution Using Water Melon (Citrillus Lanatus) Peels as Adsorbent. Open Access Journal of Chemistry. 2019;**3**(1): 1-7
16. Rajeshwar MS. Removal of Cd (II) Ions From Aqueous Solution by Adsorbtion on Activated Carbon Prepared From Lapsi (ChoerospendiasAxillaris) Seed Store. Journal of the Institute of Enineering. 2015;**II**(I): 140 – 150
17. Danbature WL, and Yila A. Preparation and Characterization of Activated Carbon from Doumpalm Nutshell and Maiganga Coal and their Adsorption Potential for Arsenic Removal. Chemical Science and engineering Research. 2020; **1**(10): 9 – 16
18. Pindiga NY, Walid AH, Abdullahi AO, and Mohammad AB. Kinetic, Equilibrium and Thermodynamic Study of the Adsorption of Pb (II) and Cd (II) Ions from Aqueous Solution by the Leaves Biomass of Guava and Cashew Plants. Online Journal of Chemistry. 2022; **2**(1): 23–38.
19. Pindiga NY, IbrahimA, Alhaji MK, and Adamu S. Adsorption Study of Methylene Blue on to Powder Activated Carbon Prepared from Ananas Cosmosus Peels. Nano Chemical Resources. 2023; **8**(4): 231-242
20. Bilal M, Ali J, Yassen-Khan M, RafiuddinKanwl F. Synthesis and Characterization of Activated Carbon From Capris Decidua for Removal of Pb(II) From Model Aqueous Solution: Kinitic and Thermodynamic Approach. Desalination and Water Treatment. 2021;**221**: 185-196